Cell Reports

Requirement for Dicer in Maintenance of Monosynaptic Sensory-Motor Circuits in the Spinal Cord

Graphical Abstract

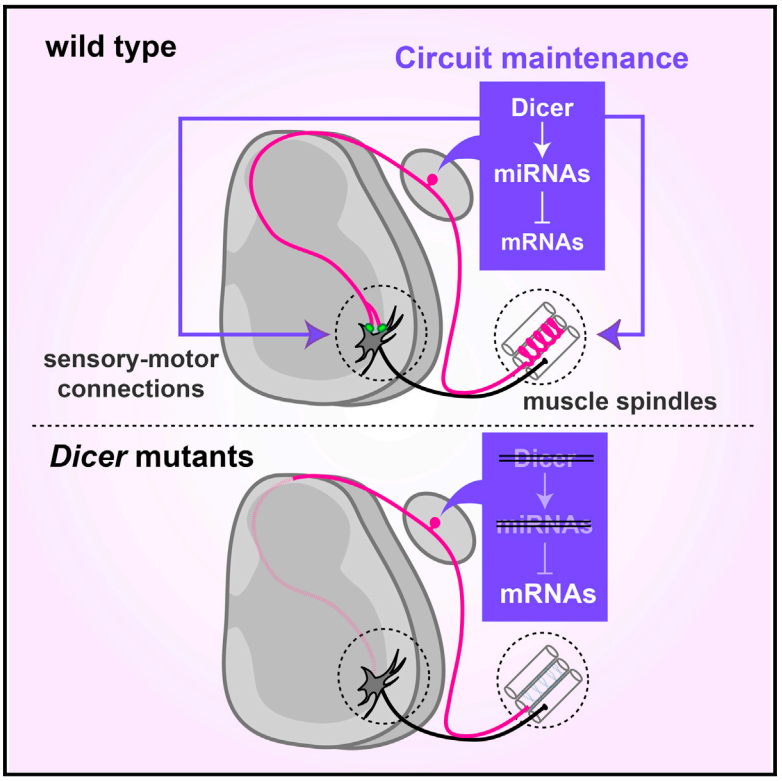

Highlights

- Deletion of *Dicer* does not cause defects in sensory-motor circuit formation
- Deletion of *Dicer* does not cause significant death of sensory neurons
- Dicer is required for maintenance of sensory-motor circuits
- Absence of Dicer changes expression of some miRNAs and mRNAs in the dorsal root ganglia

Authors

Fumiyasu Imai, Xiaoting Chen, Matthew T. Weirauch, Yutaka Yoshida

Correspondence

yutaka.yoshida@cchmc.org

In Brief

The molecular mechanisms underlying neural circuit maintenance remain unclear. Imai et al. show that deletion of *Dicer* in sensory neurons causes no obvious defects in the formation of monosynaptic sensory-motor circuits, but circuit maintenance is impaired. These studies reveal that Dicer is critical for monosynaptic sensory-motor circuit maintenance.

Imai et al., 2016, Cell Reports *17*, 2163–2172
November 22, 2016
http://dx.doi.org/10.1016/j.celrep.2016.10.083

Cell Reports
Report

Requirement for Dicer in Maintenance of Monosynaptic Sensory-Motor Circuits in the Spinal Cord

Fumiyasu Imai,[1] Xiaoting Chen,[2] Matthew T. Weirauch,[1,2,3] and Yutaka Yoshida[1,4,*]
[1]Division of Developmental Biology
[2]Center for Autoimmune Genomics and Etiology
[3]Division of Biomedical Informatics
Cincinnati Children's Hospital Medical Center, 3333 Burnet Avenue, Cincinnati, OH 45229, USA
[4]Lead Contact
*Correspondence: yutaka.yoshida@cchmc.org
http://dx.doi.org/10.1016/j.celrep.2016.10.083

SUMMARY

In contrast to our knowledge of mechanisms governing circuit formation, our understanding of how neural circuits are maintained is limited. Here, we show that Dicer, an RNaseIII protein required for processing microRNAs (miRNAs), is essential for maintenance of the spinal monosynaptic stretch reflex circuit in which group Ia proprioceptive sensory neurons form direct connections with motor neurons. In postnatal mice lacking *Dicer* in proprioceptor sensory neurons, there are no obvious defects in specificity or formation of monosynaptic sensory-motor connections. However, these circuits degrade through synapse loss and retraction of proprioceptive axonal projections from the ventral spinal cord. Peripheral terminals are also impaired without retracting from muscle targets. Interestingly, despite these central and peripheral axonal defects, proprioceptive neurons survive in the absence of Dicer-processed miRNAs. These findings reveal that Dicer, through its production of mature miRNAs, plays a key role in the maintenance of monosynaptic sensory-motor circuits.

INTRODUCTION

During nervous system development, neural circuits are typically established, refined by pruning, and then maintained throughout an animal's lifetime. We now have amassed considerable knowledge of how neural circuits are formed and refined during development (Cohen and Greenberg, 2008; Sanes and Yamagata, 2009; Shen and Scheiffele, 2010), yet we know very little about how neural circuits are maintained in the mammalian central nervous system.

The monosynaptic spinal stretch reflex arc is essential for motor behaviors and is driven by a relatively simple circuit in which group Ia proprioceptive sensory neurons, whose cell bodies are located in the dorsal root ganglia (DRGs), form monosynaptic connections with particular sets of motor neurons in the ventral spinal cord (Brown, 1981; Mears and Frank, 1997). Peripherally, group Ia afferents project axons to muscle spindles, which provide feedback to the spinal cord about the state of muscle contraction and limb position (Maier, 1997; Windhorst, 2007). Recent studies have revealed the molecular mechanisms guiding proprioceptive sensory afferent projections to the ventral spinal cord and the formation of specific connections within their target regions (Arber, 2012; Chen et al., 2003; Ladle et al., 2007; Levine et al., 2012; Catela et al., 2015). Once these monosynaptic sensory-motor circuits are formed, however, we know little about how they are maintained over the lifespan of an animal.

MicroRNAs (miRNAs) are non-coding short RNAs that control gene expression and translational regulation (Hausser and Zavolan, 2014). Immature miRNAs are transcribed from the genome and subsequently processed by the RNaseIII enzyme, Dicer (Krol et al., 2010). These mature miRNAs are essential for cell survival in various kinds of neurons in mammals (Petri et al., 2014) and have been found to be important for establishing neuronal polarity, dendritic branch elaboration, neurite outgrowth, and synaptic function in certain neuronal subsets (Davis et al., 2008; Edbauer et al., 2010; Hancock et al., 2014; Hong et al., 2013; Li et al., 2012; Muddashetty et al., 2011).

In our study of monosynaptic sensory-motor circuits, we show that Dicer, in proprioceptive sensory neurons, is not required for initial circuit formation but is essential for long-term circuit maintenance in mice.

RESULTS

Deletion of *Dicer* in Sensory Neurons Causes Sensory-Motor Circuit Defects

To determine whether roles of Dicer in sensory-motor circuits we first examined *Dicer* expression profiles in spinal cords and DRGs of newborn wild-type mice at postnatal day 0 (P0). *Dicer* was ubiquitously expressed in both the spinal cord and the DRG (Figure 1A). Although Dicer has been shown to play a role

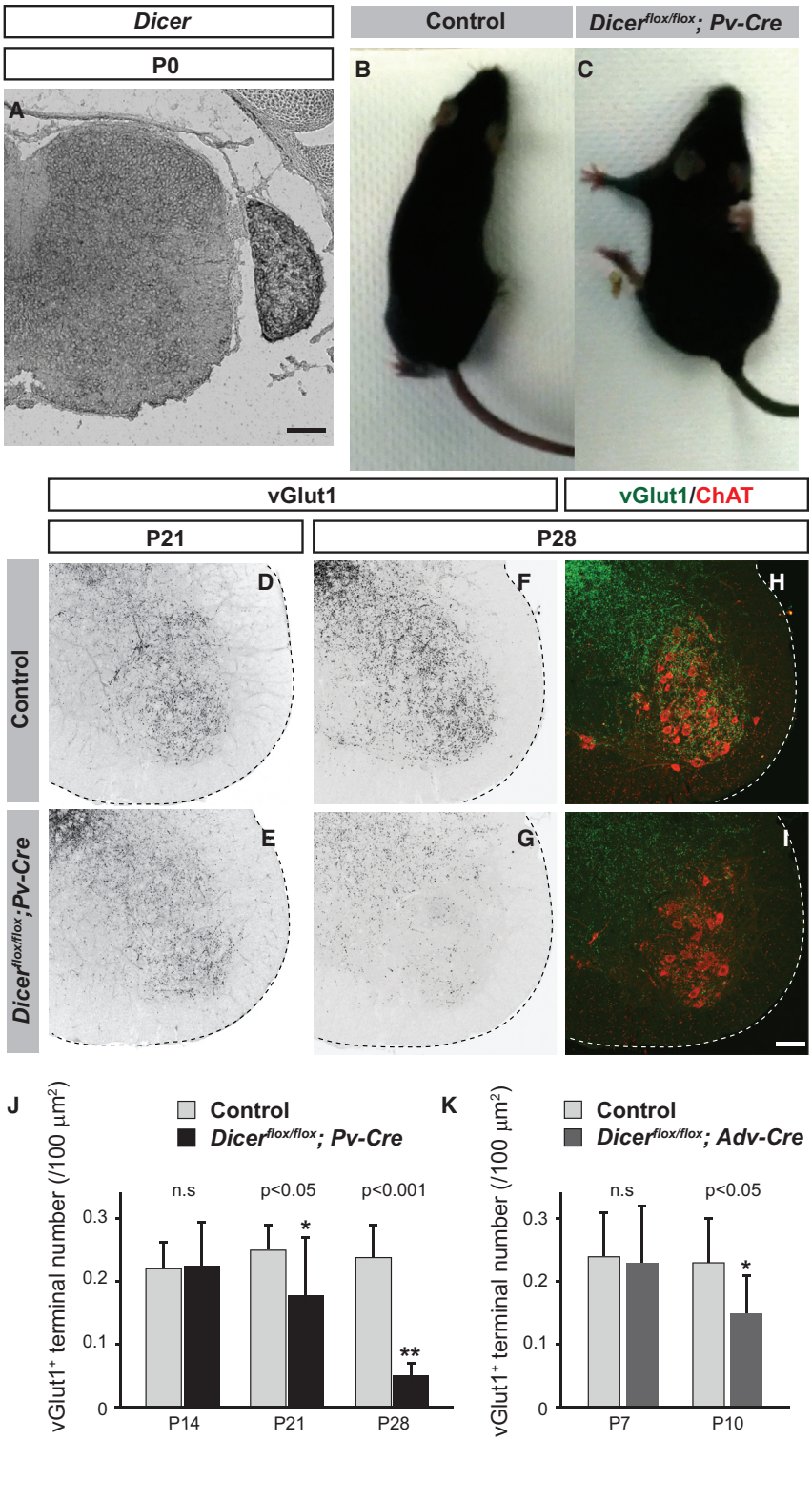

Figure 1. Loss of *Dicer* in Sensory Neurons Affects Sensory-Motor Connections

(A) In situ hybridization of *Dicer* in the spinal cord and DRG of a P0 wild-type mouse. *Dicer* is ubiquitously expressed in the spinal cord and DRG.

(B and C) P28 control (B) and $Dicer^{flox/flox}$; *Pv-Cre* (C) mice. $Dicer^{flox/flox}$; *Pv-Cre* mice show severe ataxia, extensor rigidity, and posture abnormalities.

(D–G) Immunostaining of vGlut1 in control (D and F) and $Dicer^{flox/flox}$; *Pv-Cre* (E and G) mice at P21 (D and E) and P28 (F and G).

(H and I) Immunostaining of vGlut1 (green) and ChAT (red) in control (H) and $Dicer^{flox/flox}$; *Pv-Cre* (I) mice at P28. Dotted lines outline the spinal cords.

(J and K) $vGlut1^+$ terminal number/$ChAT^+$ area from control and $Dicer^{flox/flox}$; *Pv-Cre* mice at P14, P21, and P28 (J), and from control and $Dicer^{flox/flox}$; *Adv-Cre* mice at P7 and P14 (K). *$p < 0.05$, **$p < 0.001$, Student's t test, n = 5. Scale bar: 100 μm. See also Figure S1.

Error bars represent SD.

in the neurogenesis of motor and DRG neurons (Chen et al., 2011; Huang et al., 2010; Hancock et al., 2014), it is unclear whether it functions in postmitotic motor neurons or DRG sensory neurons. In this study, we focused on proprioceptive sensory neurons. We targeted the deletion of *Dicer* in proprioceptive sensory neurons by crossing $Dicer^{flox/flox}$ mice with *parvalbumin (Pv)-Cre* mice, which exhibit restricted Cre expression in proprioceptive sensory neurons within the DRG (Harfe et al., 2005; Hippenmeyer et al., 2005). Although endogenous Pv is expressed during embryogenesis, *Pv-Cre*-mediated recombination occurs in the DRG from P0 (Lilley et al., 2013). Using in situ hybridization, we confirmed that *Dicer* mRNA was not detected in large-diameter (presumably proprioceptive) DRG neurons of P7 $Dicer^{flox/flox}$; *Pv-Cre* mice (Figures S1A–S1D). Prior to P14, $Dicer^{flox/flox}$; *Pv-Cre* mice survived without exhibiting any overt motor behavioral phenotypes. By P21, subtle behavioral deficits developed, and by P28, the mice exhibited ataxia (Figures 1B and 1C). Similar ataxic behaviors have been observed previously in mutants such as *Runx3* and *Egr3* mice that show compromised sensory-motor development (Levanon et al., 2002; Tourtellotte and Milbrandt, 1998; Inoue et al., 2002), suggesting that $Dicer^{flox/flox}$; *Pv-Cre* mice may have similar sensory-motor circuit defects. We first visualized the proprioceptive sensory terminals in the ventral spinal cords of the *Dicer* mutants by immunostaining for vesicular glutamate receptor 1 (vGlut1) (Oliveira et al., 2003; Alvarez et al., 2004) (Figures 1D–1I). No obvious differences in the number of $vGlut1^+$ terminals in the ventral spinal cord were observed

between control and *Dicer*$^{flox/flox}$; *Pv-Cre* mice at P14 (Figure 1J; data not shown). However, in the *Dicer* mutants, the number of vGlut1$^+$ proprioceptive sensory terminals was progressively reduced compared to controls from P21 to P28 (Figures 1D–1J), without any changes in ChAT$^+$ motor neuron numbers, locations, or areas within the ventral spinal cord (Figures 1H, 1I, and S1K; data not shown). Similarly, in P50 *Dicer*$^{flox/flox}$; *Pv-Cre* mice, vGlut1$^+$ sensory terminals were almost completely absent in the ventral spinal cord (Figures S2A and S2B). Taken together, the decrease in vGlut1$^+$ sensory terminals was consistent with the timing of behavioral deficits observed in *Dicer*$^{flox/flox}$; *Pv-Cre* mice.

Since Pv is expressed in various regions of the brain (Celio, 1990), it was possible that changes in the brain rather than the spinal cord of *Dicer*$^{flox/flox}$; *Pv-Cre* mice could have caused the behavioral phenotypes. To investigate this possibility, we used another Cre mouse line, *Advillin (Adv)-Cre*, in which Cre is expressed as early as embryonic day 12.5 (E12.5) in sensory neurons in the DRG and trigeminal ganglia, but it is not expressed in any other regions of the brain or spinal cord (Hasegawa et al., 2007). *Dicer*$^{flox/flox}$; *Adv-Cre* mice showed similar reductions in vGlut1$^+$ proprioceptive terminals in the ventral spinal cord (Figures 1K and S1E–S1J) as well as similar behavioral deficits as early as P10. *Dicer*$^{flox/flox}$; *Adv-Cre* mice typically died of unknown causes around P14. Despite the timing differences in phenotype progression, these data strongly suggest that the behavioral deficits in *Dicer*$^{flox/flox}$; *Pv-Cre* and *Dicer*$^{flox/flox}$; *Adv-Cre* mice are caused by disruptions in sensory-motor circuits and not by compromised higher brain circuits.

Loss of Dicer Causes Retraction of Central Projections of Proprioceptive Sensory Neurons without Significant Neuronal Cell Death

To further characterize the effects of *Dicer* deletion on monosynaptic sensory-motor circuits, we determined Dicer's effects on cell survival and proprioceptive axon morphology. To track cell survival, we monitored the expression of TrkC, a proprioceptive sensory neuron marker (Klein et al., 1994), in proprioceptive cell bodies. At P14 and P21, the numbers of TrkC$^+$ DRG neurons were similar between control and *Dicer*$^{flox/flox}$; *Pv-Cre* mice, but at P28, those were reduced in *Dicer*$^{flox/flox}$; *Pv-Cre* mice (Figures 2A–2C). The number of apoptotic proprioceptive neurons was slightly but significantly increased in *Dicer*$^{flox/flox}$; *Pv-Cre* mice at P21 and P28 over the control mice (Figures S2E–S2I); however, by P50, it appeared that the numbers of proprioceptive sensory neurons were similar in *Dicer*$^{flox/flox}$; *Pv-Cre* and control mice (Figures S2C and S2D). In *Dicer*$^{flox/flox}$; *Adv-Cre* mice, we did not find any reductions in TrkC$^+$ DRG neurons at P10 (Figure 2D) when these mice exhibited ataxia. Therefore, strong reductions in vGlut1$^+$ terminals do not appear to be explained by proprioceptive sensory neuron cell death in *Dicer*$^{flox/flox}$; *Pv-Cre* or *Dicer*$^{flox/flox}$; *Adv-Cre* mice.

Next, we examined the central projections of proprioceptive sensory neurons in *Dicer*$^{flox/flox}$; *Pv-Cre* mice. To visualize the axons, we injected Neurobiotin into dorsal roots (Clarke et al., 2011) to label both cutaneous and proprioceptive axons (Figures 2E–2G). In control mice, Neurobiotin$^+$ cutaneous and proprioceptive sensory axons projected to the dorsal and ventral horns of the spinal cord, respectively (Figures 2E and 2G). In contrast, in *Dicer*$^{flox/flox}$; *Pv-Cre* mice, Neurobiotin$^+$ sensory axons were detected only in the dorsal, but not the ventral, spinal cord (Figures 2F–2H), indicating that proprioceptive axons had retracted from the ventral spinal cord. We also found that Pv$^+$ sensory axons had similarly retracted from the ventral horn in *Dicer*$^{flox/flox}$; *Adv-Cre* mice at P10 (Figures 2I and 2J). Despite the loss in ventral axonal projections, the *Dicer*$^{flox/flox}$; *Adv-Cre* mice showed no obvious differences in vGlut1$^+$ synapse densities (vGlut1$^+$ terminal numbers/Pv$^+$ axon volume) compared to control mice at P10, suggesting that axon and synapse losses occurred concurrently in *Dicer*$^{flox/flox}$; *Adv-Cre* mice (Figures 2K–2M). Taken together, these data demonstrate that the vGlut1$^+$ proprioceptive sensory terminals had decreased in the ventral spinal cord in proportion with the reduction in proprioceptive axonal density in the ventral horn in *Dicer* mutant mice. Importantly, these processes occurred in the absence of significant sensory neuron cell death.

Defective Peripheral Axonal Terminations of Ia Proprioceptive Sensory Neurons in *Dicer* Mutant Mice

We then examined the peripheral projections of group Ia proprioceptive sensory neurons at their target muscle spindles. To visualize the group Ia terminals at the muscle spindle, we crossed *Dicer*$^{flox/flox}$; *Pv-Cre* with *Thy1-GFP* transgenic mice (Feng et al., 2000), in which GFP is expressed by motor and sensory neurons (Zhang et al., 2015). GFP$^+$ Ia axons innervated Egr3$^+$ intrafusal muscle fibers in control and *Dicer*$^{flox/flox}$; *Pv-Cre* mice at P21 (Figures 3A and 3B), but the total number of axons was largely reduced in *Dicer*$^{flox/flox}$; *Pv-Cre* mice in the rectus femoris muscle at P21 and P28 (Figure 3E). P28 *Dicer*$^{flox/flox}$; *Pv-Cre* mice rarely exhibited clear GFP$^+$ Ia afferent terminals. Instead, they showed an aberrant morphology lacking typical Ia afferent axonal terminal patterns (Figure 3D). Egr3$^+$ intrafusal muscle fibers appeared intact in these mutants, but they lacked innervation by GFP$^+$ Ia axons (Figure 3D). Interestingly, some Ia afferents did not retract from the muscle (Figure 3D). We found a similar array of defects in *Dicer*$^{flox/flox}$; *Adv-Cre* mice at P10 (Figure 3F; data not shown). Last, in a set of control experiments, we did not find any defects in motor axon innervation of neuromuscular junctions in P28 *Dicer*$^{flox/flox}$; *Pv-Cre* mice (Figures 3G–3J). These data reveal that Dicer is required for maintenance of group Ia proprioceptive sensory afferent terminations in target muscle spindles.

Defects in Proprioceptive Peripheral Projections in *Dicer* Mutants Do Not Likely Cause Deficits in the Central Terminals of Proprioceptive Sensory Neurons

Because muscle spindle-derived neurotrophic factor 3 (NT-3) has been shown to affect monosynaptic sensory-motor connections (Mentis et al., 2011; Shneider et al., 2009), it was possible that defects in retrograde signaling from muscle spindles to proprioceptive sensory neurons in *Dicer* mutants caused deficits in the central terminals of proprioceptive sensory neurons. To test this possibility, we transected the sciatic nerve in P7 wild-type mice and analyzed sensory-motor connections at various time

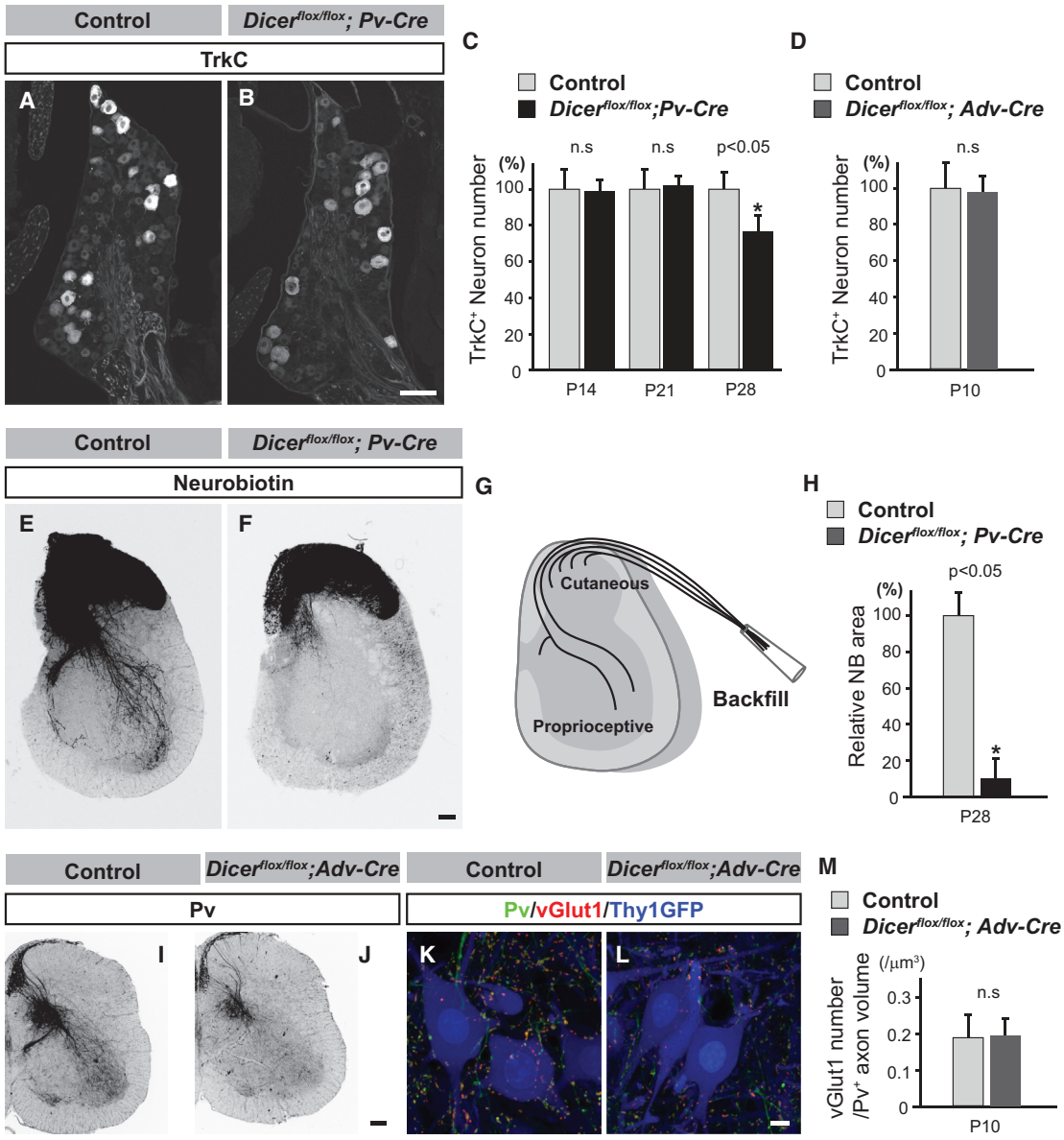

Figure 2. Loss of *Dicer* in Sensory Neurons Affects Proprioceptive Central Axon Projections

(A and B) Immunostaining of TrkC in DRGs of control (A) and *Dicer*$^{flox/flox}$; *Pv-Cre* (B) mice at P28.

(C and D) Relative TrkC^{+} neuron number from control and *Dicer*$^{flox/flox}$; *Pv-Cre* mice at P14, P21, and P28 (C), and from control and *Dicer*$^{flox/flox}$; *Adv-Cre* mice at P10 (D). *p < 0.05, Student's t test, n = 5.

(E and F) Central projections of DRG neurons were visualized by Neurobiotin backfills in control (E) and *Dicer*$^{flox/flox}$; *Pv-Cre* (F) mice at P28.

(G) Schematic representation of the Neurobiotin backfill method. Central projections of all DRG neurons are labeled by Neurobiotin. Cutaneous and proprioceptive sensory axons project to the dorsal and ventral spinal cord, respectively.

(H) Relative Neurobiotin (NB)$^{+}$ axon area in the ventral spinal cords of P28 control and *Dicer*$^{flox/flox}$; *Pv-Cre* mice. *p < 0.05, Student's t test, n = 4.

(I and J) Immunostaining of Pv from spinal cords of control (I) and *Dicer*$^{flox/flox}$; *Adv-Cre* mice (J) at P10.

(K and L) Immunostaining of Pv (green), vGlut1 (red), and GFP (blue, Thy1-GFP) from the ventral spinal cords of control (K) and *Dicer*$^{flox/flox}$; *Adv-Cre* mice (L) at P10.

(M) Quantification of vGlut1^{+} terminal number per Pv^{+}axon volume (per cubic micrometer) in P10 control and *Dicer*$^{flox/flox}$; *Adv-Cre* mice. No significant differences were observed (Student's t test, n = 4). Scale bar: 100 μm (B, F, and J), 10 μm (L). See also Figure S2.

Error bars represent SD.

points (Figure 3K). There were no significant differences in vGlut1^{+} terminal numbers at P21 (postinjury day 14), and vGlut1^{+} terminal number decreased only from P28 (Figure 3L). These data suggest that defects in retrograde signaling from the peripheral muscles are unlikely to contribute to the proprioceptive sensory terminal deficits in *Dicer* mutants.

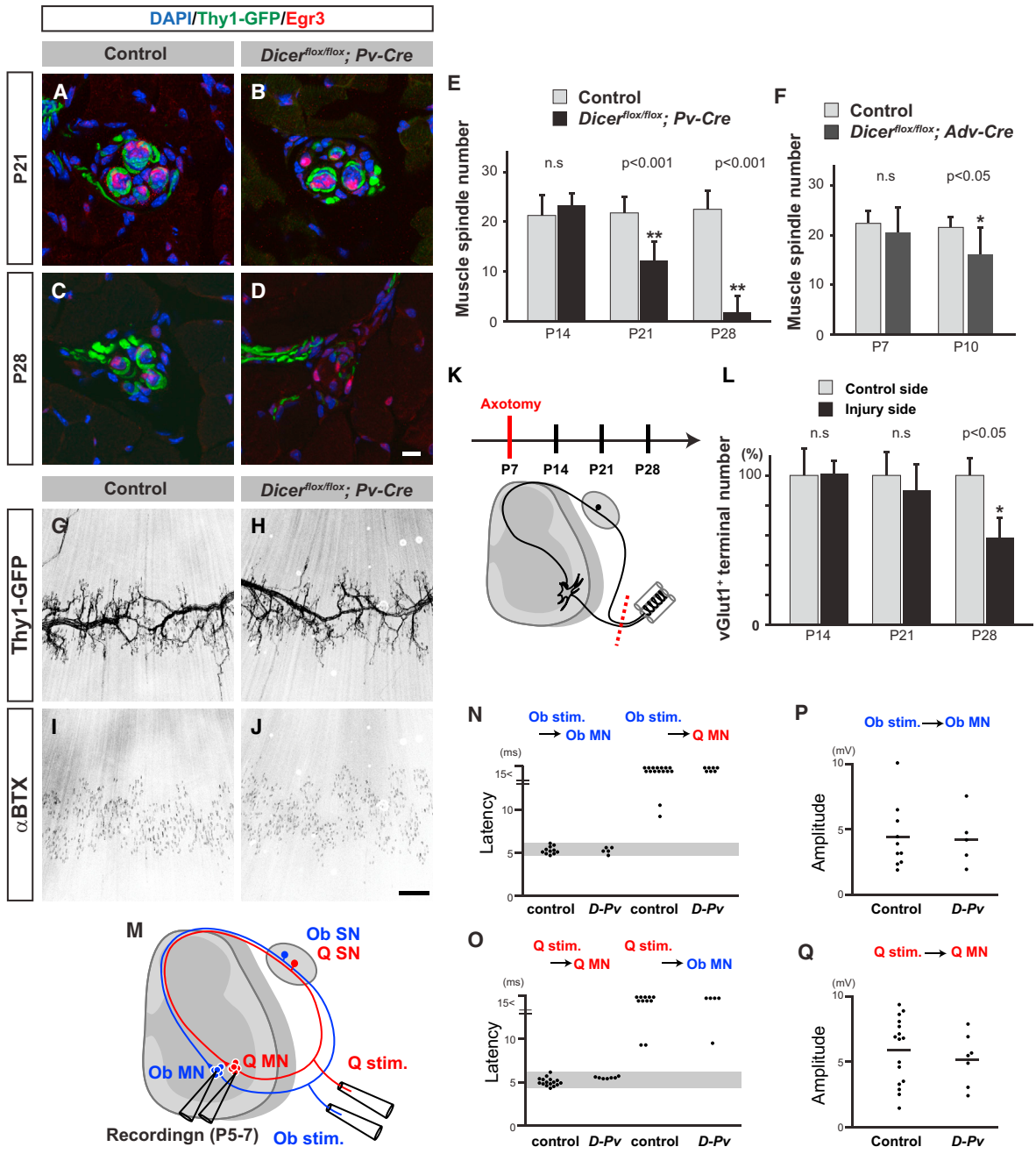

Figure 3. Loss of *Dicer* in Proprioceptive Sensory Neurons Affects Muscle Spindle Structure

(A–D) Muscle spindles were labeled by GFP (green, Thy1-GFP), Egr3 (red), and DAPI (blue) from rectus femoris muscles of control (A and C) and *Dicer*$^{flox/flox}$; *Pv-Cre* (B and D) at P21 (A and B) and P28 (C and D).

(E and F) Quantification of muscle spindle numbers from rectus femoris muscles of control and *Dicer*$^{flox/flox}$; *Pv-Cre* (E), and *Dicer*$^{flox/flox}$; *Adv-Cre* mice (F). *p < 0.05, **p < 0.01, Student's t test, n = 5.

(G–J) Motor axons and neuromuscular junctions were labeled by Thy1-GFP (G and H) and tetramethylrhodamine α-bungarotoxin (αBTX) (I and J) in gluteus muscles of control (G and I) and *Dicer*$^{flox/flox}$; *Pv-Cre* mice (H and J) at P28.

(K) Schematic drawing of the peripheral axotomy experiment. Nerves were transected at P7 and analyzed at P14, P21, and P28.

(L) Relative vGlut1$^+$ terminal number between control and injury sides of ventral spinal cords taken from P14, P21, and P28 wild-type mice. *p < 0.05, Student's t test, n = 4.

(legend continued on next page)

No Obvious Defects in the Establishment of Sensory-Motor Reflex Circuits in *Dicer* Mutant Mice

Our data suggest that in *Dicer*$^{flox/flox}$; *Pv-Cre* mice, monosynaptic sensory-motor circuits are initially formed, but not maintained after P14. To address whether initial sensory-motor circuits are functional in terms of synaptic specificity and formation, we focused on the obturator and quadriceps sensory-motor reflex arcs. Proprioceptive Ia afferents form monosynaptic connections with motor neurons innervating the same or synergistic muscles but not antagonistic muscles (Frank and Mendelson, 1990). Previous studies have shown that Ia afferents conveying sensory information from either obturator or quadriceps nerves do not form synaptic contacts on motor neurons supplying the opposite muscles (Mears and Frank, 1997). We performed intracellular recordings from obturator and quadriceps motor neurons following obturator and quadriceps sensory nerve stimulation, respectively (Figure 3M), using short-latency input recordings to identify the monosynaptic sensory-motor responses. In control mice, latencies of homonymous connections, obturator-to-obturator and quadriceps-to-quadriceps, ranged between 4.9–6.1 and 4.3–6.2 ms, respectively (gray bins in Figures 3N and 3O), which were similar to the latencies recorded from *Dicer*$^{flox/flox}$; *Pv-Cre* mice (Figures 3N and 3O), suggesting that these connections are monosynaptic. The amplitudes of monosynaptic excitatory postsynaptic potentials (EPSPs) were measured from recordings from the obturator and quadriceps motor neurons after obturator and quadriceps sensory nerve stimulation, respectively. The EPSP amplitudes of *Dicer*$^{flox/flox}$; *Pv-Cre* mice were similar to those observed in control mice (Figures 3P and 3Q). Therefore, these data indicate that obturator and quadriceps sensory afferents properly form monosynaptic connections with homonymous motor neurons in *Dicer*$^{flox/flox}$; *Pv-Cre* mice.

We then examined whether Dicer is involved in establishing the synaptic specificity of monosynaptic sensory-motor connections by recording from obturator motor neurons following quadriceps nerve stimulation or from quadriceps motor neurons following obturator nerve stimulation. We did not find any aberrant monosynaptic connections in these antagonistic sensory-motor connection pairs in both littermate control and *Dicer*$^{flox/flox}$; *Pv-Cre* mice (Figures 3N and 3O). Taken together, these data indicate that Dicer does not regulate the specificity or formation of obturator and quadriceps sensory-motor reflex circuits.

Downstream Targets of Dicer Activity

To deduce the molecular logic of sensory-motor circuit maintenance regulated by Dicer, we analyzed both miRNAs and mRNAs in control and *Dicer* mutant mice by RNA sequencing (RNA-seq) analysis. First, we compared miRNA expression patterns in DRGs of control and *Dicer*$^{flox/flox}$; *Pv-Cre* mice at P21 (Figure 4A). Expression of some miRNAs such as mir-486 and -3107 were unchanged, whereas other miRNAs showed approximately 20%–30% reductions in *Dicer* mutants compared to control mice (Figure 4A). For instance, *mir-127* was highly expressed in the DRG and showed a 30% reduction in *Dicer*$^{flox/flox}$; *Pv-Cre* mice (Figure 4A). The miRNAs with only reduced expression in *Dicer* mutants suggests that they are expressed in both proprioceptive and cutaneous sensory neurons in the DRG. To determine whether *mir-127* expression is indeed decreased in proprioceptive sensory neurons of *Dicer* mutant mice, we examined *mir-127* expression (Figures 4B–4F). *mir-127* was highly expressed in most DRG neurons at P7 and P21 (Figures 4B and 4E). Most large-diameter NeuN^{+} neurons (which are presumably proprioceptive sensory neurons) lacked *mir-127* expression in *Dicer*$^{flox/flox}$; *Pv-Cre* mice at P21 (dotted lines in Figures 4F and 4F′). In contrast, small-diameter neurons (which are presumably cutaneous sensory neurons) still expressed *mir-127* in *Dicer*$^{flox/flox}$; *Pv-Cre* mice (arrow in Figure 4F). In *Dicer*$^{flox/flox}$; *Adv-Cre* mice, both large- and small-diameter NeuN^{+} neurons lacked *mir-127* expression (Figure 4C; dotted lines in Figures 4D and 4D′ for large-diameter NeuN^{+} neuron). Taken together, these data indicate that *mir-127* is expressed in both proprioceptive and cutaneous sensory neurons in the DRG, and *Dicer* deletion affects maturation of these miRNAs.

To determine the direct and indirect target genes of these miRNAs, we analyzed mRNA gene expression profiles in the DRG, comparing *Dicer*$^{flox/flox}$; *Adv-Cre* (P10) and *Dicer*$^{flox/flox}$; *Pv-Cre* (P21) mutant mice with control mice (P10 or P21). We examined all genes expressed in the DRG (fragments per kilobase of transcript per million mapped reads [FPKM] > 3) and plotted the fold changes in gene expression over the levels in control mice (Figures 4G and 4H). From these plots, we identified sets of upregulated (fold change > 150%, $p < 0.05$, green areas) and downregulated genes (fold change < 75%, $p < 0.05$, purple areas) in both *Dicer*$^{flox/flox}$; *Adv-Cre* and *Dicer*$^{flox/flox}$; *Pv-Cre* mice (Figure 4I). Gene ontology (GO) enrichment analysis of upregulated genes suggests that many of these genes are associated with the extracellular matrix or involved in growth factor binding (Figure S3K). For example, vitronectin (Vtn) expression was upregulated in the DRG of *Dicer* mutants (225% and 339% in *Dicer*$^{flox/flox}$; *Adv-Cre* and Dicer$^{flox/flox}$; *Pv-Cre* mice compared to control mice, respectively; Figures S3I and S3J). Expression of proprioceptor-specific genes, *Pv/Pvalb* and *Er81/Etv1*, were reduced in both *Dicer*$^{flox/flox}$; *Adv-Cre* and *Dicer*$^{flox/flox}$; *Pv-Cre* mice, respectively (Figures S3C, S3D, S3G, and S3H). Conversely, *TrkC (Ntrk3)* and *Runx3* were only slightly decreased in *Dicer*$^{flox/flox}$; *Adv-Cre* and *Dicer*$^{flox/flox}$; *Pv-Cre* mice, respectively, compared to controls (Figures S3A, S3B, S3E, and S3F).

(M) Schematic representation of intracellular recordings from motor neurons following muscle nerve stimulation. Obturator (Ob) (blue) and quadriceps (Q) (red) motor neurons (MNs) were identified by antidromic responses following obturator and quadriceps sensory nerve stimulation (Ob stim. and Q stim.), respectively. (N and O) Quantification of the shortest latencies of EPSP onset from individual Q motor neuron recordings with Ob stimulation (N) and Ob motor neuron recordings with Q stimulation (O) in control and *Dicer*$^{flox/flox}$; *Pv-Cre* (*D-Pv*) mice. Monosynaptic ranges (gray bins) were defined by homonymous connections (recordings of Ob motor neurons with Ob nerve stimulation or Q motor neuron recordings with Q nerve stimulation) in control mice.
(P and Q) Quantification of amplitudes of homonymous monosynaptic EPSPs from Ob (P) and Q motor neurons (Q). Scale bar: 10 μm (D), 500 μm (J).
Error bars represent SD.

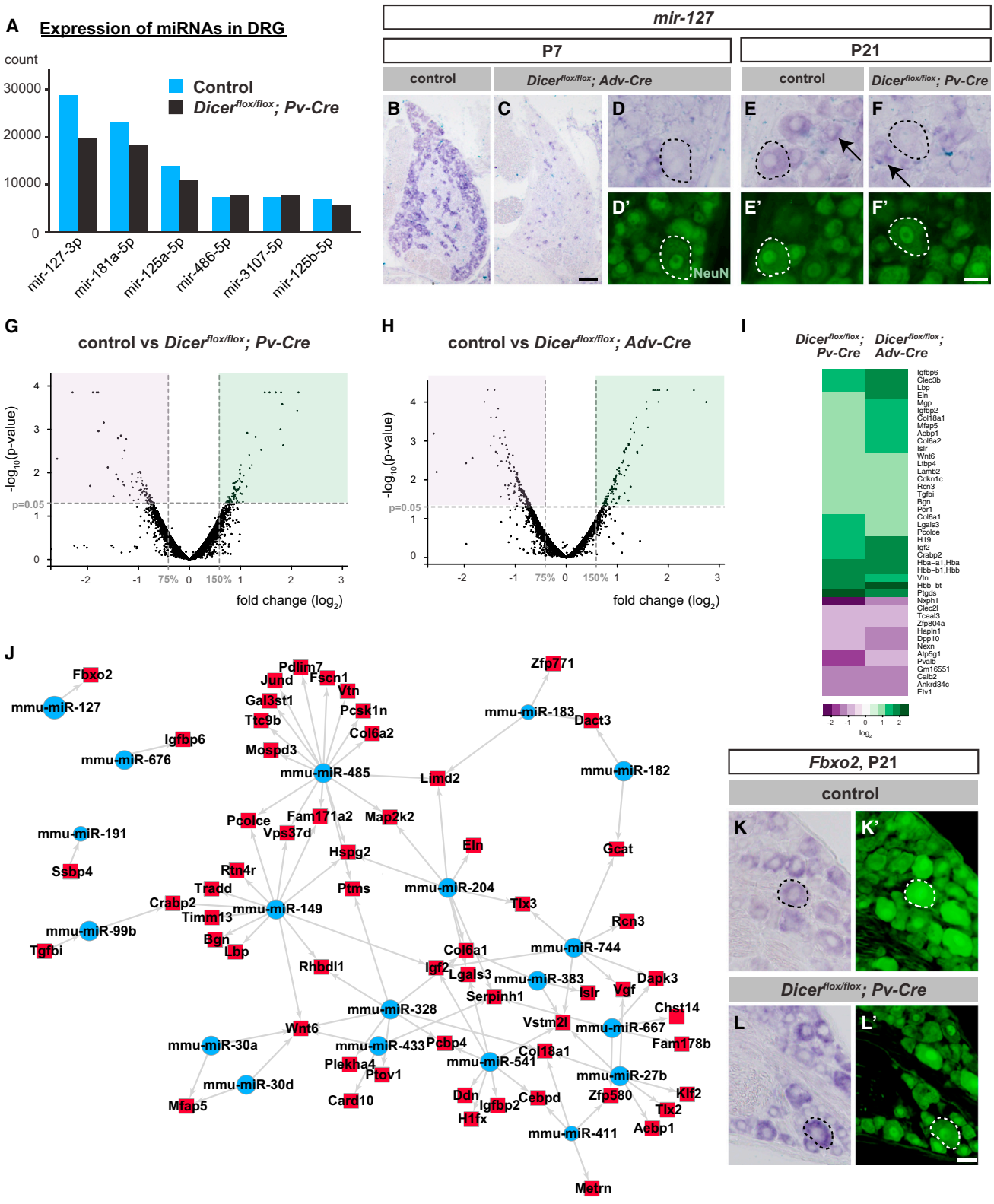

(legend on next page)

To identify potential direct targets of these miRNAs, we searched for putative binding sites in the 3′-UTRs of genes upregulated in *Dicer*$^{flox/flox}$; *Pv-Cre* mice (Figure 4J). First, we selected the 50 most abundant miRNAs in the DRGs of control mice, which collectively represented over 90% of all the DRG miRNAs, and found that 35 of those miRNAs were downregulated in *Dicer*$^{flox/flox}$; *Pv-Cre* DRGs (Figure 4A). We then examined the 3′-UTRs of upregulated mRNA sequences in *Dicer*$^{flox/flox}$; *Pv-Cre* DRGs for putative binding sites for those 35 miRNAs. In total, we identified almost 60 potential direct miRNA gene targets (red boxes in Figure 4J). In situ hybridization experiments revealed that expression of *F-box only protein 2* (*Fbxo2*), a potential target of *mir-127*, was upregulated in large-diameter NeuN$^+$ neurons in the DRGs of *Dicer*$^{flox/flox}$; *Pv-Cre* mice compared to controls (Figures 4K and 4L).

DISCUSSION

Monosynaptic sensory-motor circuits have been extensively studied using electrophysiology, mouse genetics, and molecular approaches since the 1950s (Brown, 1981; Arber, 2012; Ladle et al., 2007; Catela et al., 2015). However, how these and all other circuits in the nervous system are properly maintained over the lifespan of an animal is unclear. Our studies using mutant mice show that Dicer, expressed by proprioceptive sensory neurons, is required for the maintenance of sensory-motor circuits. In our *Dicer* mutant mice, sensory-motor and peripheral defects arose simultaneously, raising the possibility that the peripheral deficits disrupted the intracellular transport of important muscle spindle-derived signaling molecules. To test this, we performed peripheral axon transections on P7 wild-type mice to intentionally block intracellular transport. However, sensory-motor connections were affected only after a 21-day lag postsurgery (Figure 3), indicating that disrupted signaling from the periphery is likely not causing the central deficits in *Dicer* mutants. Alternatively, it could be that proprioceptive central defects immediately affect the peripheral projections of proprioceptive sensory neurons in *Dicer* mutants, or that Dicer may simultaneously regulate maintenance of both central and peripheral axons of proprioceptive sensory neurons.

To uncover some of the Dicer-regulated mechanisms underlying circuit maintenance, we examined miRNAs in the DRG that had diminished expression in the *Dicer* mutants, and also searched for upregulated and downregulated genes. The reduced expression of *Er81* in proprioceptors in *Dicer* mice was of particular interest, because Ia proprioceptive sensory axons in *Er81* mutants fail to reach the ventral spinal cord (Arber et al., 2000). In the absence of Dicer, proprioceptive group Ia neurons may start losing their overall proprioceptive transcriptional identities, which could then lead to the altered axonal phenotypes observed in *Dicer* mutant mice.

Our RNA-seq analyses also identified several miRNAs that might promote the upkeep of neural circuits. Because miRNAs regulate not only mRNA stability but also translation, *Dicer* deletion may cause differences in protein expression without affecting mRNA levels (a scenario that would not have been detected in our RNA-seq analyses). Therefore, further examination of these miRNAs, including *miRNA-127*, *-182*, and *-183*, their target genes, and the resulting proteomes of *Dicer*-depleted proprioceptive sensory neurons, will provide useful insights into whether miRNAs function to control gene or protein expression of molecules essential for preserving monosynaptic sensory-motor circuits.

Our studies suggest that neural circuit maintenance is an active process requiring a precise transcriptional program. However, what types of extrinsic and/or intrinsic signaling pathways are involved, and which mechanisms promote circuit stability over the lifetime of an animal? A delicate balance must be struck between the need for circuit preservation and the ability to alter neural circuitry in response to stress and injury. Finally, a greater understanding of circuit maintenance may provide new inroads toward preventing circuit degeneration via bolstering circuit maintenance mechanisms in patients suffering from neurodegenerative disease.

EXPERIMENTAL PROCEDURES

Mice

The following mouse lines were used: *Dicer*-floxed (Harfe et al., 2005), *Pv-Cre* (Hippenmeyer et al., 2005), *Adv-Cre* (Hasegawa et al., 2007), and *Thy1-GFP* (Feng et al., 2000) mice. Mouse handling and procedures were approved by the Institutional Animal Care and Use Committee at the Cincinnati Children's Hospital Research Foundation.

Tissue Preparation

Spinal cords and DRGs were fixed in 4% paraformaldehyde (PFA)/phosphate buffer (PB) for 2 hr for immunohistochemistry or overnight for in situ hybridization. Afterward, they were vibratome sectioned at 100–200 μm or cryostat sectioned at 10–20 μm.

In Situ Hybridizations

In situ hybridizations were performed according to standard protocols (Imai et al., 2016). Template DNAs were cloned into the pCRII vector (Life Technologies) by PCR using the following primers: 5′-GACGACTTCCTGGAG TATGACC-3′, 5′-TATCAGGTGGTTGAGGGTTTTC-3′ for *Dicer* mRNA (Figure 1); 5′-GAATGGAAGATGCCCAAGAA-3′, 5′-GAGGGTTTTCTCTGCGCT

Figure 4. Potential Downstream Targets of Dicer-Mediated Pathways

(A) Expression profiles of miRNAs in the DRGs of control and *Dicer*$^{flox/flox}$; *Pv-Cre* mice at P21.

(B–F) In situ hybridization of *mir-127* in DRGs of P7 control (B), *Dicer*$^{flox/flox}$; *Adv-Cre* (C and D) mice, and P21 control (E) and *Dicer*$^{flox/flox}$; *Pv-Cre* (F) mice. (D′)–(F′) show NeuN (green) staining of images (D)–(F). Dotted lines indicate large-diameter NeuN$^+$ neurons. Arrows indicate mir-127$^+$ small-diameter NeuN$^+$ neurons. A limited number of small-diameter neurons still expressed *mir-127* in *Dicer*$^{flox/flox}$; *Adv-Cre* mice (C and D).

(G and H) Plots of mRNA fold-change differences (log_2) versus p values (log_{10}) of control versus *Dicer*$^{flox/flox}$; *Pv-Cre* mice at P21 (G) and control versus and *Dicer*$^{flox/flox}$; *Adv-Cre* at P10 (H). Green areas show upregulated genes ($p < 0.05$, >150%), whereas purple areas show downregulated genes ($p < 0.05$, <75%).

(I) Upregulated and downregulated genes in both *Dicer*$^{flox/flox}$; *Pv-Cre* and *Dicer*$^{flox/flox}$; *Adv-Cre* mice.

(J) Network map showing putative regulatory relationships between miRNAs (blue circles) and mRNAs (red squares).

(K and L) In situ hybridizations of *Fbxo2* in DRGs of P21 control (K) and *Dicer*$^{flox/flox}$; *Pv-Cre* (L) mice. (K′) and (L′) show NeuN (green) staining of images (K) and (L). Dotted lines indicate large-diameter NeuN$^+$ neurons. Scale bar: 100 μm (C), 10 μm (F′ and L′). See also Figure S3 and Tables S1, S2, and S3.

CTG-3′ for *Dicer* mRNA (exon 23, for Figure S1). For *mir*-127, we used DIG-labeled LNA probes (Exiqon).

Immunohistochemistry

Cryosections or vibratome sections were stained with the following primary antibodies: anti-vGlut1 (Millipore; AB5905), anti-ChAT (Millipore; AB144), anti-TrkC (R&D Systems; AF1404), anti-Pv (Swant; PV27), and anti-Egr3 (Santa Cruz Biotechnology; SC-191). For TrkC staining, cryosections were heated in 10 mM sodium citrate (pH 6.0). Images were scanned with a Nikon A1R confocal microscope. Quantification of vGlut1$^+$ terminals was performed with IMARIS (Bitplane) software.

Neurobiotin Axonal Labeling

To label sensory axons, hemisected spinal cords were incubated in a recirculating artificial cerebrospinal fluid (aCSF) bath containing NaCl (127 mM), KCl (1.9 mM), KH_2PO_4 (1.2 mM), $CaCl_2$ (2 mM), $MgSO_4$ (1 mM), $NaHCO_3$ (26 mM), and D-glucose (20.5 mM), that was oxygenated. Dorsal roots were placed in glass pipettes filled with Neurobiotin (Vector Laboratories) overnight. Neurobiotin was visualized with Alexa 488-conjugated streptavidin (Life Technologies).

Whole-Mount Muscle Staining

Gluteus and rectus femoris muscles were taken from Thy1-GFP$^+$ mice and fixed in 4% PFA/PB overnight. Afterward, muscles were incubated with tetramethylrhodamine-α-bungarotoxin (Life Technologies).

Intracellular Recordings

Dissections of spinal cords and electrophysiological recordings have been previously described in detail (Imai et al., 2016; Fukuhara et al., 2013). Briefly, spinal cords from P5–P7 newborn pups were hemisectioned in oxygenated aCSF bath. Nerves were stimulated with 10-mA, 0.001-ms pulses. Intracellular potentials were recorded using glass micropipettes filled with 2 M potassium acetate with 0.5% Fastgreen and 300 mM lidocaine *N*-ethyl bromide. Synaptic potentials were recorded 20–60 times (1 Hz) and averaged. Obturator or quadriceps motor neurons were identified by antidromic activation.

Gene Expression and Data Analysis

DRGs were taken from control and *Dicer*$^{flox/flox}$; *Adv-Cre* mice at P10 or control and *Dicer*$^{flox/flox}$; *Pv-Cre* mice at P21. RNA was isolated using the RNeasy kit (QIAGEN). RNA-seq was performed on an Illumina HiSeq 2500 sequencing system. Sequencing data were mapped using TopHat and analyzed with CuffLinks (Trapnell et al., 2012; Lewis et al., 2005). To find putative miRNA target sequences, we used mouse miRNA gene target predictions available in the TargetScanMouse database (release 6.2) (Lewis et al., 2005). The network map depicted in Figure 4 was created using Cytoscape software (Shannon et al., 2003).

Statistical Analysis

Statistical evaluation was performed using Student's t test, and values are shown as mean ± SD. $p < 0.05$ is considered significant.

SUPPLEMENTAL INFORMATION

Supplemental Information includes three figures and three tables and can be found with this article online at http://dx.doi.org/10.1016/j.celrep.2016.10.083.

AUTHOR CONTRIBUTIONS

F.I. and Y.Y. designed the project. F.I. performed experiments and analyzed data. X.C. and M.T.W. analyzed miRNA target sequence data. F.I., M.T.W., and Y.Y. wrote the manuscript.

ACKNOWLEDGMENTS

We thank T. Cope (Georgia Institute of Technology); S. Crone, N. Gross, and S. Rommer (Cincinnati Children's Hospital Medical Center [CCHMC]); and E. Demireva (Michigan State University) for providing comments on the manuscript. We also thank F. Wang (Duke University) and S. Arber (University of Basel) for providing *Advillin-Cre* and *Pv-Cre* mice, respectively. We are grateful to S. Nikolaou and R. Cornwall (CCHMC) for help with muscle spindle labeling, N. Salomonis (CCHMC) for help with RNA-seq analysis, and M. Kofron (CCHMC) for help with confocal microscope analyses. We also thank the members of the Y.Y. laboratory for helpful discussions regarding these experiments. This work is supported by NINDS-NS093002 (Y.Y.).

Received: June 25, 2015
Revised: August 8, 2016
Accepted: October 24, 2016
Published: November 22, 2016

REFERENCES

Alvarez, F.J., Villalba, R.M., Zerda, R., and Schneider, S.P. (2004). Vesicular glutamate transporters in the spinal cord, with special reference to sensory primary afferent synapses. J. Comp. Neurol. *472*, 257–280.

Arber, S., Ladle, D.R., Lin, J.H., Frank, E., and Jessell, T.M. (2000). ETS gene Er81 controls the formation of functional connections between group Ia sensory afferents and motor neurons. Cell *101*, 485–498.

Arber, S. (2012). Motor circuits in action: specification, connectivity, and function. Neuron *74*, 975–989.

Brown, A.G. (1981). Organization in the Spinal Cord (Springer).

Catela, C., Shin, M.M., and Dasen, J.S. (2015). Assembly and function of spinal circuits for motor control. Annu. Rev. Cell Dev. Biol. *31*, 669–698.

Celio, M.R. (1990). Calbindin D-28k and parvalbumin in the rat nervous system. Neuroscience *35*, 375–475.

Chen, H.H., Hippenmeyer, S., Arber, S., and Frank, E. (2003). Development of the monosynaptic stretch reflex circuit. Curr. Opin. Neurobiol. *13*, 96–102.

Chen, J.A., Huang, Y.P., Mazzoni, E.O., Tan, G.C., Zavadil, J., and Wichterle, H. (2011). Mir-17-3p controls spinal neural progenitor patterning by regulating Olig2/Irx3 cross-repressive loop. Neuron *69*, 721–735.

Clarke, J.N., Anderson, R.L., Haberberger, R.V., and Gibbins, I.L. (2011). Non-peptidergic small diameter primary afferents expressing VGluT2 project to lamina I of mouse spinal dorsal horn. Mol. Pain *7*, 95.

Cohen, S., and Greenberg, M.E. (2008). Communication between the synapse and the nucleus in neuronal development, plasticity, and disease. Annu. Rev. Cell Dev. Biol. *24*, 183–209.

Davis, T.H., Cuellar, T.L., Koch, S.M., Barker, A.J., Harfe, B.D., McManus, M.T., and Ullian, E.M. (2008). Conditional loss of Dicer disrupts cellular and tissue morphogenesis in the cortex and hippocampus. J. Neurosci. *28*, 4322–4330.

Edbauer, D., Neilson, J.R., Foster, K.A., Wang, C.F., Seeburg, D.P., Batterton, M.N., Tada, T., Dolan, B.M., Sharp, P.A., and Sheng, M. (2010). Regulation of synaptic structure and function by FMRP-associated microRNAs miR-125b and miR-132. Neuron *65*, 373–384.

Feng, G., Mellor, R.H., Bernstein, M., Keller-Peck, C., Nguyen, Q.T., Wallace, M., Nerbonne, J.M., Lichtman, J.W., and Sanes, J.R. (2000). Imaging neuronal subsets in transgenic mice expressing multiple spectral variants of GFP. Neuron *28*, 41–51.

Frank, E., and Mendelson, B. (1990). Specification of synaptic connections between sensory and motor neurons in the developing spinal cord. J. Neurobiol. *21*, 33–50.

Fukuhara, K., Imai, F., Ladle, D.R., Katayama, K., Leslie, J.R., Arber, S., Jessell, T.M., and Yoshida, Y. (2013). Specificity of monosynaptic sensory-motor connections imposed by repellent Sema3E-PlexinD1 signaling. Cell Rep. *5*, 748–758.

Hancock, M.L., Preitner, N., Quan, J., and Flanagan, J.G. (2014). MicroRNA-132 is enriched in developing axons, locally regulates Rasa1 mRNA, and promotes axon extension. J. Neurosci. *34*, 66–78.

Harfe, B.D., McManus, M.T., Mansfield, J.H., Hornstein, E., and Tabin, C.J. (2005). The RNaseIII enzyme Dicer is required for morphogenesis but not patterning of the vertebrate limb. Proc. Natl. Acad. Sci. USA *102*, 10898–10903.

Hasegawa, H., Abbott, S., Han, B.X., Qi, Y., and Wang, F. (2007). Analyzing somatosensory axon projections with the sensory neuron-specific Advillin gene. J. Neurosci. *27*, 14404–14414.

Hausser, J., and Zavolan, M. (2014). Identification and consequences of miRNA-target interactions—beyond repression of gene expression. Nat. Rev. Genet. *15*, 599–612.

Hippenmeyer, S., Vrieseling, E., Sigrist, M., Portmann, T., Laengle, C., Ladle, D.R., and Arber, S. (2005). A developmental switch in the response of DRG neurons to ETS transcription factor signaling. PLoS Biol. *3*, e159.

Hong, J., Zhang, H., Kawase-Koga, Y., and Sun, T. (2013). MicroRNA function is required for neurite outgrowth of mature neurons in the mouse postnatal cerebral cortex. Front. Cell. Neurosci. *7*, 151.

Huang, T., Liu, Y., Huang, M., Zhao, X., and Cheng, L. (2010). Wnt1-cre-mediated conditional loss of Dicer results in malformation of the midbrain and cerebellum and failure of neural crest and dopaminergic differentiation in mice. J. Mol. Cell Biol. *2*, 152–163.

Imai, F., Ladle, D.R., Leslie, J.R., Duan, X., Rizvi, T.A., Ciraolo, G.M., Zheng, Y., and Yoshida, Y. (2016). Synapse formation in monosynaptic sensory-motor connections is regulated by presynaptic Rho GTPase Cdc42. J. Neurosci. *36*, 5724–5735.

Inoue, K., Ozaki, S., Shiga, T., Ito, K., Masuda, T., Okado, N., Iseda, T., Kawaguchi, S., Ogawa, M., Bae, S.C., et al. (2002). Runx3 controls the axonal projection of proprioceptive dorsal root ganglion neurons. Nat. Neurosci. *5*, 946–954.

Klein, R., Silos-Santiago, I., Smeyne, R.J., Lira, S.A., Brambilla, R., Bryant, S., Zhang, L., Snider, W.D., and Barbacid, M. (1994). Disruption of the neurotrophin-3 receptor gene trkC eliminates la muscle afferents and results in abnormal movements. Nature *368*, 249–251.

Krol, J., Loedige, I., and Filipowicz, W. (2010). The widespread regulation of microRNA biogenesis, function and decay. Nat. Rev. Genet. *11*, 597–610.

Ladle, D.R., Pecho-Vrieseling, E., and Arber, S. (2007). Assembly of motor circuits in the spinal cord: driven to function by genetic and experience-dependent mechanisms. Neuron *56*, 270–283.

Levanon, D., Bettoun, D., Harris-Cerruti, C., Woolf, E., Negreanu, V., Eilam, R., Bernstein, Y., Goldenberg, D., Xiao, C., Fliegauf, M., et al. (2002). The Runx3 transcription factor regulates development and survival of TrkC dorsal root ganglia neurons. EMBO J. *21*, 3454–3463.

Levine, A.J., Lewallen, K.A., and Pfaff, S.L. (2012). Spatial organization of cortical and spinal neurons controlling motor behavior. Curr. Opin. Neurobiol. *22*, 812–821.

Lewis, B.P., Burge, C.B., and Bartel, D.P. (2005). Conserved seed pairing, often flanked by adenosines, indicates that thousands of human genes are microRNA targets. Cell *120*, 15–20.

Li, Z., He, X., and Feng, J. (2012). Dicer is essential for neuronal polarity. Int. J. Dev. Neurosci. *30*, 607–611.

Lilley, B.N., Pan, Y.A., and Sanes, J.R. (2013). SAD kinases sculpt axonal arbors of sensory neurons through long- and short-term responses to neurotrophin signals. Neuron *79*, 39–53.

Maier, A. (1997). Development and regeneration of muscle spindles in mammals and birds. Int. J. Dev. Biol. *41*, 1–17.

Mears, S.C., and Frank, E. (1997). Formation of specific monosynaptic connections between muscle spindle afferents and motoneurons in the mouse. J. Neurosci. *17*, 3128–3135.

Mentis, G.Z., Blivis, D., Liu, W., Drobac, E., Crowder, M.E., Kong, L., Alvarez, F.J., Sumner, C.J., and O'Donovan, M.J. (2011). Early functional impairment of sensory-motor connectivity in a mouse model of spinal muscular atrophy. Neuron *69*, 453–467.

Muddashetty, R.S., Nalavadi, V.C., Gross, C., Yao, X., Xing, L., Laur, O., Warren, S.T., and Bassell, G.J. (2011). Reversible inhibition of PSD-95 mRNA translation by miR-125a, FMRP phosphorylation, and mGluR signaling. Mol. Cell *42*, 673–688.

Oliveira, A.L., Hydling, F., Olsson, E., Shi, T., Edwards, R.H., Fujiyama, F., Kaneko, T., Hökfelt, T., Cullheim, S., and Meister, B. (2003). Cellular localization of three vesicular glutamate transporter mRNAs and proteins in rat spinal cord and dorsal root ganglia. Synapse *50*, 117–129.

Petri, R., Malmevik, J., Fasching, L., Åkerblom, M., and Jakobsson, J. (2014). miRNAs in brain development. Exp. Cell Res. *321*, 84–89.

Sanes, J.R., and Yamagata, M. (2009). Many paths to synaptic specificity. Annu. Rev. Cell Dev. Biol. *25*, 161–195.

Shannon, P., Markiel, A., Ozier, O., Baliga, N.S., Wang, J.T., Ramage, D., Amin, N., Schwikowski, B., and Ideker, T. (2003). Cytoscape: a software environment for integrated models of biomolecular interaction networks. Genome Res. *13*, 2498–2504.

Shen, K., and Scheiffele, P. (2010). Genetics and cell biology of building specific synaptic connectivity. Annu. Rev. Neurosci. *33*, 473–507.

Shneider, N.A., Mentis, G.Z., Schustak, J., and O'Donovan, M.J. (2009). Functionally reduced sensorimotor connections form with normal specificity despite abnormal muscle spindle development: the role of spindle-derived neurotrophin 3. J. Neurosci. *29*, 4719–4735.

Tourtellotte, W.G., and Milbrandt, J. (1998). Sensory ataxia and muscle spindle agenesis in mice lacking the transcription factor Egr3. Nat. Genet. *20*, 87–91.

Trapnell, C., Roberts, A., Goff, L., Pertea, G., Kim, D., Kelley, D.R., Pimentel, H., Salzberg, S.L., Rinn, J.L., and Pachter, L. (2012). Differential gene and transcript expression analysis of RNA-seq experiments with TopHat and Cufflinks. Nat. Protoc. *7*, 562–578.

Windhorst, U. (2007). Muscle proprioceptive feedback and spinal networks. Brain Res. Bull. *73*, 155–202.

Zhang, Y., Lin, S., Karakatsani, A., Rüegg, M.A., and Kröger, S. (2015). Differential regulation of AChR clustering in the polar and equatorial region of murine muscle spindles. Eur. J. Neurosci. *41*, 69–78.